Spectroscopic and imaging performance of DEPFET pixel sensors[1]

J. Ulrici[2,3], S.Adler[3], P. Buchholz[4], P. Fischer[3], P. Klein[4], M. Löcker[3], G. Lutz[5], W. Neeser[3], L. Strüder[6], M. Trimpl[4], N. Wermes[3]

[3] *Physikalisches Institut der Universität Bonn, Nußallee 12, D-53115 Bonn, Germany*

[4] *Physikalisches Institut der Universität Dortmund, D-44221 Dortmund, Germany*

[5] *Max-Planck-Institut für Physik, Föhriger Ring 6, D-80805 München, Germany*

[6] *Max-Planck-Institut für extraterristrische Physik, Gießenbachstraße, D-85740 Garching, Germany*

Abstract

DEPFET pixel sensors consist of a p-channel JFET directly integrated into a high-ohmic n-silicon substrate. They offer a very low noise performance at room temperature and are therefore of interest for applications in biomedicine, x-ray astronomy and particle physics. Measurements on single pixel devices demonstrating the low noise potential of DEPFET sensors are shown. The DEPFET pixel bioscope system is based on a 64x64 matrix of DEPFET pixels. Measurements of the homogeneity of the charge collection efficiency and of the spatial resolution of the system as well as on the capability of DEPFET sensors to detect tritium with a good efficiency are presented.

.

1. Introduction

The principal idea of the DEPFET (DEPleted Field Effect Transistor) sensor is the integration of the first amplifying transistor into the sensor itself [1]. Stray capacitances due to connections between sensor and amplifier are therefore avoided and a very small input capacitance can be accomplished. The result is a very low noise performance.

While several monolithic pixel sensors have been proposed and realized on a prototype level [2-3], the DEPFET concept has been continuously developed in the recent years and matured to a certain level [4-7].

In our case, the first amplifying transistor is a p-channel JFET with an annular structure having the source in the center. The sensor material consists of a 300 µm thick, fully depleted, high resistivity silicon substrate.

The detector works as follows (Fig. 1): By sidewards depletion [8] and an additional n-implantation below the JFET, a potential minimum for electrons is created underneath the transistor channel [4]. This can be considered as an internal gate of the JFET. The backside of the device has been optimized for low-energy radiation detection. It consists of a p+ implant and a passivation layer resulting in a 200 nm thin entrance window. A particle entering the detector from the backside creates electron-hole pairs. While

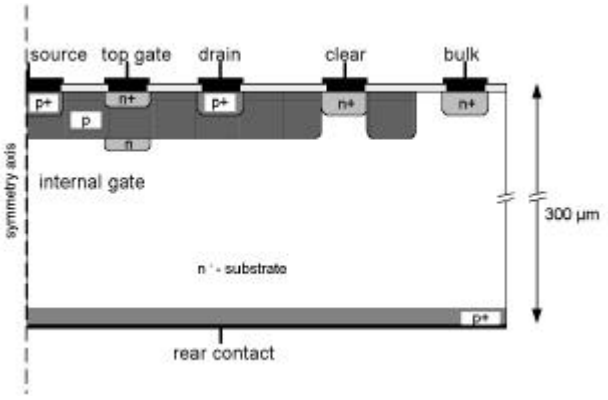

Fig. 1 Cross section of DEPFET pixel. The symmetry axis of the annular transistor is in the source.

[1]Work supported by the Deutsche Forschungsgesellschaft (DFG) under contract WE 976/2-1 and by the Ministerium für Wissenschaft und Forschung des Landes Nordrhein-Westfalen under contract IV A5 - 10600198

[2]Corresponding author, mailing address: Physikalisches Institut, Nußallee 12, D-53115 Bonn, Germany; Phone: +49 (228) 732352; Fax: +49 (228) 733220; e-mail: ulrici@physik.uni-bonn.de;

the holes drift into the rear contact of the detector, the electrons are collected in the internal gate where they are stored. The signal charge thus leads to a change in the potential of the internal gate, resulting in a modulation of the channel current of the JFET.

The internal gate of the transistor is filled up with signal as well as with thermally generated charges, which have to be removed from time to time. This can be accomplished by applying a positive voltage pulse to an additional n-type contact next to the transistor, also referred to as the clear contact.

Since in DEPFET pixel sensors the signal charge is stored in the pixel cell, a pixel does not need to be read out continuously. Compared to other pixel sensor concepts, this can be used to significantly reduce the number of readout channels, avoiding bump bonding and resulting in a small scale readout chip. The readout principle of an array of DEPFET pixels as well as the system setup of the DEPFET bioscope system, which operates a full DEPFET matrix of 64x64 pixels, will be described later in this paper.

For DEPFET single pixel devices, an excellent low-noise performance at room temperature has already been reported [7]. Further measurements showing an even better noise performance will be presented here.

The very thin entrance window at the backside of the device and the low noise properties of DEPFET sensors allow the detection of tritium which is often used in autoradiography as a radioactive tracer. Measurements demonstrating the detection of ^{3}H as well as measurements of the homogeneity of the charge collection and of the spatial resolution of the DEPFET matrix are shown.

2. Operation of a full DEPFET pixel array

In Fig. 2, a section of an array of DEPFET pixels with a square geometry of 50 x 50 μm^2 is shown. The gate, source and clear contacts of the pixels are connected to each other row-wise by aluminium traces. They are contacted by wire bonds at the edges of the sensor matrix. The p-implantations of the drains of the transistors are connected column-wise and can be contacted at the bottom of the matrix.

By switching the pixels on and off row-wise by applying a voltage to the external gates of the JFETs and by reading

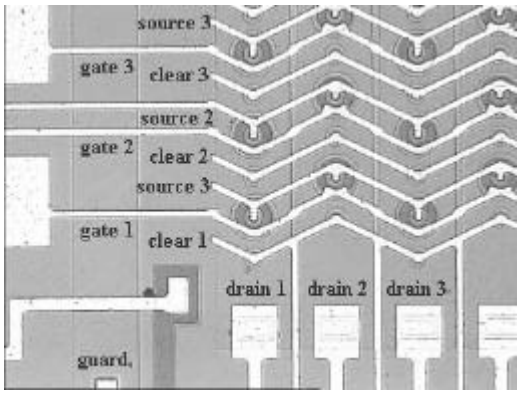

Fig. 2 Section of DEPFET array with square pixels.

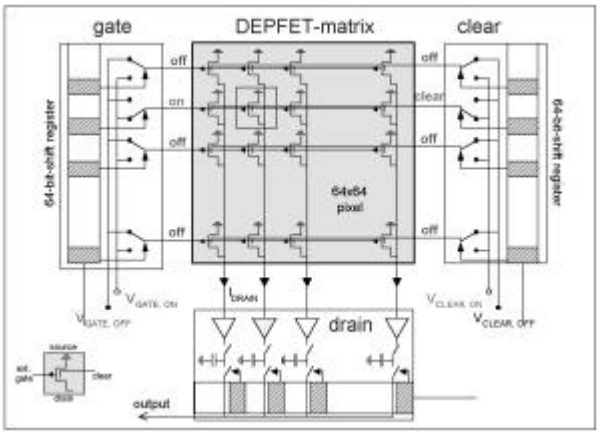

Fig. 3 Principle of operation of a full DEPFET pixel array

them out column-wise, the pixels in the matrix can be randomly accessed (Fig. 3). A full readout cycle of a matrix of DEPFET pixels then for each row of pixels can be described as follows: The pixels are reset by emptying the internal gate and their pedestal currents are recorded. After a certain integration time, their signal currents are measured. The difference between signal and pedestal current depends on the amount of collected charge in the internal gate.

The DEPFET pixel bioscope realizes the operation of such an array of 64 x 64 DEPFET pixels and was mainly developed for applications in autoradiography. An image of the system setup is shown in Fig. 4; a more detailed description can be found in [6]. In the bioscope, the on/off

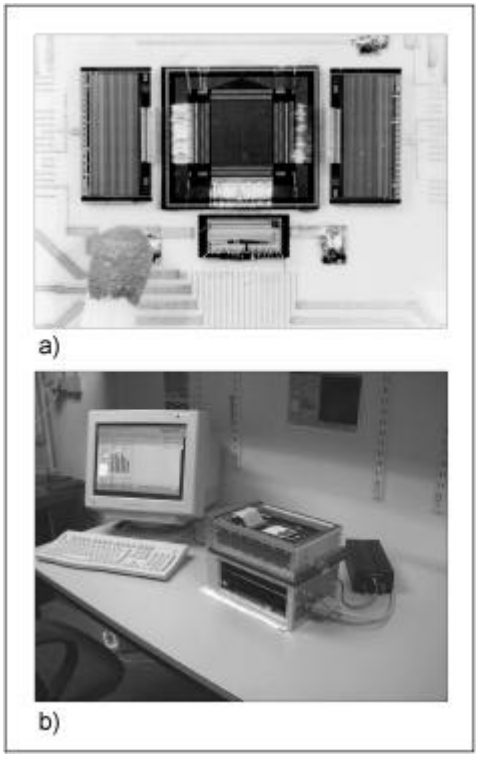

Fig. 4 a) Image of a DEPFET Hybrid with a 64x64 DEPFET-Matrix and the ASICs SWITCHER and CARLOS b) The DEPFET pixel Bioscope System

switching of the pixels as well as the row-wise clearing of the pixels is realized by a dedicated ASIC, called SWITCHER. The low-noise readout and amplification of signal and pedestal currents is accomplished by a second dedicated ASIC, called CARLOS [9]. Both ASICs are mounted on a hybrid ceramic and wire bonded to the DEPFET pixel matrix. The analog data is digitized with a 12 bit ADC on a dedicated PCB; the data acquisition as well as the communication with a PC is controlled by a digital PCB using XILINX FPGAs.

3. Measurements on Single Pixel Devices

The low noise potential of DEPFET pixels was studied with single isolated pixel devices. The detector is irradiated from its front side with a ^{55}Fe-source. Because the X-rays have a mean range of 30 µm in silicon, the width of the charge cloud is smaller than when irradiating the sensor from the backside, resulting in less split events.

The current signal of the JFET is converted into a voltage signal and preamplified on a dedicated low-noise PCB. The signal is then shaped with an ORTEC shaper before being digitized and analyzed with an 8k channel MCA.

Fig. 5 shows an ^{55}Fe spectrum recorded at a shaping time of 10µs at room temperature. One can see the k_α-line at 5,89 keV, the k_β-line at 6,49 keV and the photo escape peak at 4,15 keV. The low energy tail is due to split events caused by charge sharing of the pixel with its environment, which also causes a slight asymmetry of the peaks. From the noise peak an equivalent electronic noise of ENC = (4,8 ± 0,1) e^- can be extracted. The energy resolution (FWHM) of (146 ± 8) eV at 6 keV can be determined from a Gauss fit to the k_α-Peak and is dominated by the Fano noise contribution of (14,2 ± 0,3) e^- [7]. The SNR (Signal to Noise Ratio) at 6 keV measured at room temperature is thus (96 ± 4).

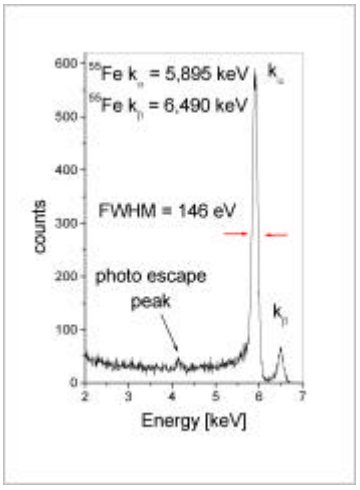

Fig. 5 ^{55}Fe-spectrum taken at room temperature.

4. Measurements on a full DEPFET pixel array

a) Homogeneity of charge collection

In order to evaluate the homogeneity of charge collection in the matrix, a laser scan across the whole matrix was carried out (Fig. 6). A laser (635 nm) with a spot size of a few µm was focused on the backside of the detector. The figure shows the response of 7 adjacent pixels to the laser signal as well as the total added signal of all pixels. Since the pixels having square geometry were staggered by half the pixel size, some of the pixels share the signal charge with a neighbour and therefore record a smaller signal amplitude; the sum of the signals in adjacent pixels, however, remains the same.

Charge loss into clear contacts, as measured in earlier generations of DEPFET detectors [5], does not occur within 5%, the value being due to the uncertainty in the amount of deposited charge.

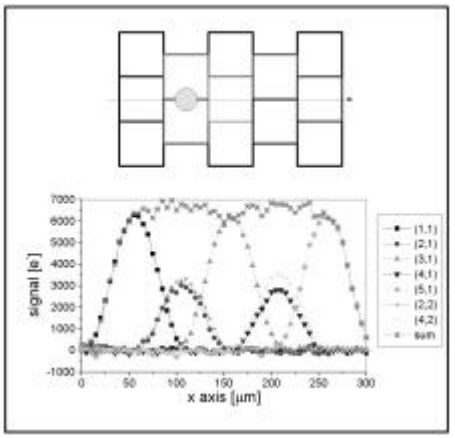

Fig. 6 Laser scan across an area of the DEPFET pixel matrix. Note the bricked layout of the pixels

b) Spatial resolution

Fig. 7 shows an image of a toothed wheel with a diameter of 1,2 mm, which was placed on the backside of the 3,2 x 3,2 mm^2 detector. The left image is obtained when no amplitude information but only the binary hit information is used. In the right image, a simple linear interpolation between the signal amplitudes of adjacent pixels was carried out to improve the spatial resolution. The black spacings between neighbouring pixels are not due to a lower sensitivity of the detector in these regions. In fact, the reason is that in a linear interpolation the charge cloud is assumed to be rectangular, such that events near the pixel edges are associated with a point closer to the pixel center. In the future, the linear interpolation will be replaced by a gaussian one.

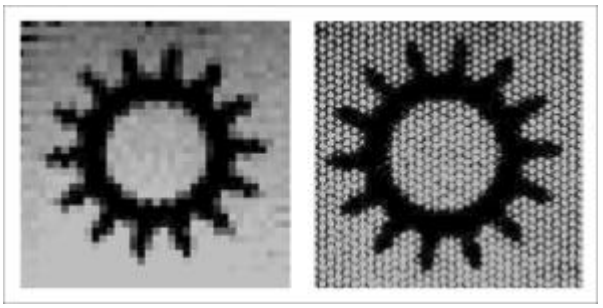

Fig. 7 Image of toothed wheel of a watch with a diameter of 1,2 mm. The left image carries only the binary information, while in the right image, charge sharing is used to perform a linear interpolation.

In order to measure the spatial resolution of the system, a 75µm thick tungsten MTF (Modulation Transfer Function) test chart was placed on the backside of the detector (Fig. 8). Having a length of 1mm, the width of the lines as well as the spacing between them was 25 µm for the most narrow ones and 50 µm, 75µm and 100µm for the broader ones, respectively. The detector was illuminated from its backside with an ^{55}Fe-source.

The function describing the intensity distribution around the edges of the lines is an error function. The width of the gaussian obtained after differentiating this distribution is given by the spatial resolution of the system. With this method, a spatial resolution of (9,4 ± 0,5) µm was determined. This corresponds to a resolution of $MTF_{0,3}$ = 27 LP/mm at the 30% point of the MTF function.

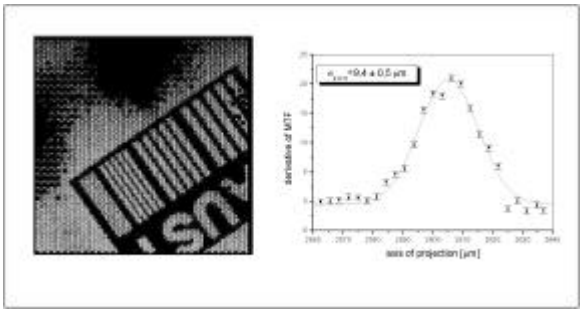

Fig. 8 Image of an MTF test chart. On the right hand side one can see the derivation of the hit distribution around one of the line edges.

c) Tritium detection

In biomedical applications, tritium is widely used as radioactive tracer. Its detection with silicon detectors, however, is somewhat problematic, since it has a very short mean range of only 800 nm in silicon. Due to the 200 nm thick entrance window at the backside of the device as well as to its low noise properties, DEPFET detectors are capable of a ^{3}H online detection, as can be seen in Fig. 9.

A commercial ^{3}H microscale* was placed on the backside of the detector. The tritium is located in the white areas of the microscale, while the dark areas are not radioactively marked. To make sure that all detected events are due to ^{3}H decays and not to noise hits, the threshold of the system was set to 9σ of the system noise.

In the right image of Fig. 9, the detected events after several hours of exposure are shown. Obviously, there were hits detected under the active regions of the microscale where the tritium was located but none in the inactive regions. A tritium detection efficiency of about 13% could be estimated for the DEPFET bioscope system using the method of Puertolas et al. [11].

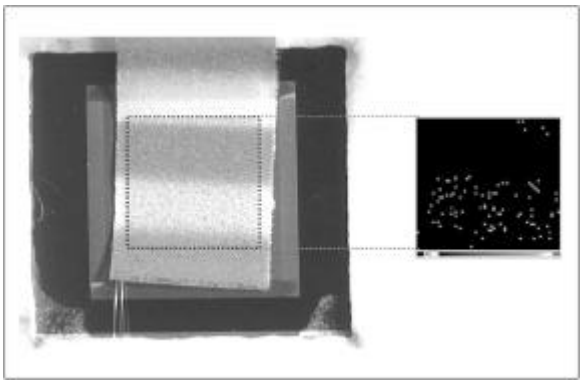

Fig. 9 Hitmap after several hours of exposition of the DEPFET matrix to a tritium microscale. The white areas of the microscale are marked with tritium.

5. Conclusions

The low noise potential of DEPFET pixel sensors has been shown in measurements with single, isolated DEPFET pixels, having an ENC= 4,8 e^- at a shaping time of 10 µs at room temperature. These low noise properties of DEPFET sensors lead to a very good energy resolution and allow the detection of low energy radiation.

With the DEPFET bioscope system, a full DEPFET matrix consisting of 4096 pixels was examined. Since the signal charge is stored in the pixels, a readout concept could be realized which avoids an expensive bump bonding technique as well as a large scale readout chip.

The charge collection efficiency was measured to be homogeneous to at least 95 %. Using a simple linear interpolation of the signal information of adjacent pixels, the spatial resolution of the DEPFET matrix was measured to be (9,4 ± 0,5) µm or 27 LP/mm, respectively. Due to the 200 nm thick entrance window at the backside of the device as well as to the low noise properties of DEPFET sensors, tritium β-decays have been detected with an efficiency of 13%; only scintillator based systems, which however have a poorer spatial resolution, offer a higher detection efficiency. The same properties of DEPFET sensors also allow

* ^{3}H-microscale RPA510, Amersham Pharmacia Biotech Europe GmbH, Munzinger Str. 9, D-70111 Freiburg, Germany

the detection of low energy X-ray radiation, which is important for applications in X-ray astronomy. In the future, time resolved measurements with biological samples as well as with different radioactive tracers are planned.

Based on these encouraging results, a further development of active pixel sensors based on the DEPFET concept is pursued for applications in X-ray astronomy [12] and particle physics [13] as well as for biomedical applications [7].

6. Acknowledgements

We would like to thank Walter Ockenfels for technical support, Giacomo Comes for CAD system administration and Dieter Gebauer for fabrication of the hybrid ceramics.

7. References

[1] J. Kemmer, G. Lutz, Nucl. Instr. And Meth. A 253 (1987) 365.
[2] C. Kenney, S. Parker, V. Peterson, W. Snoeys, J. Plummer, and C. H. Aw, Nucl. Instr. and Meth. A 342 (1994) 59
[3] W. Dulinski, talk given at the Pix 2000 conference in Genova, paper to be published in Nucl. Instr. and Meth. A. (2000)
[4] G.Cesura, N. Findeis, D. Hauff, N.Hörnel, J. Kemmer, P. Klein, P. Lechner, G. Lutz, R. Richter, H. Seitz, Nucl. Instr. and Meth. A 377 (1996) 521.
[5] P. Fischer, J. Kemmer, P. Klein, M. Löcker, G. Lutz, W. Neeser, L. Strüder, N. Wermes, preprint Bonn HE 99-08, accepted by Nucl. Instr. and Meth. A. (1999)
[6] W. Neeser, M. Böcker, P. Buchholz, P. Fischer, P. Holl, P. Klein, H. Koch, M. Löcker, G. Lutz, H. Matthäy, L. Strüder, M. Trimpl, J. Ulrici, N. Wermes, submitted to Nucl. Instr. and Meth. A.
[7] P. Klein, T. Aurisch, P. Buchholz, P. Fischer, M. Löcker, W. Neeser, L. Strüder, M. Trimpl, J.Ulrici, J. Vocht, N. Wermes, submitted to Nucl. Instr. and Meth. A.
[8] E.Gatti, P.Rehak, Nucl. Instr. and Meth. A 225 (1984) 608.
[9] P. Fischer, W.Neeser, in preparation to be submitted to Nucl. Instr. and Meth. A (2000)
[10] F. Perotti, C. Fiorini, Nucl. Instr. and Meth. A 423 (1999) 356
[11] D. Puertolas, D. Piedigrossi, H. Leutz, T. Gys, C. D'Ambrosio, IEEE Trans. on Nucl. Sci. 43 (1996) 2477
[12] P. Holl, P. Fischer, P. Klein, G. Lutz, W. Neeser, L. Strüder, N. Wermes, submitted to IEEE Trans. on Nucl. Sci. (1999)
[13] G. Lutz, talk given at 237. Heräus Seminar on Semiconductor Radia tion Detectors (2000), unpublished